Published in final edited form as:
Biopolymers. 2003 December ; 70(4): 585–594. doi:10.1002/bip.10501.

Fluorescence Properties of Labeled Proteins Near Silver Colloid Surfaces

Badri P. Maliwal, **Joanna Malicka**, **Ignacy Gryczynski**, **Zygmunt Gryczynski**, and **Joseph R. Lakowicz**
Center for Fluorescence Spectroscopy, University of Maryland at Baltimore, Department of Biochemistry and Molecular Biology, 725 West Lombard Street, Baltimore, MD 21201

Abstract

The fluorescence properties of a monolayer of labeled avidin molecules were studied near silver island films. We first adsorbed a monolayer of biotinylated-BSA as a base that was used to capture labeled avidin molecules. For labeled avidin on silver island films, we observed an increase of the fluorescence intensity of between 18 and 80 with one-photon excitation and up to several hundredfold or larger with two-photon excitation. The probes were moderately more photostable in the presence of silver islands. There was also a dramatic decrease in the lifetimes with the amplitude-weighted values decreasing from 7- to 35-fold. The data suggest that these spectral changes are due to both increased rates of excitation near the metallic particles and increases in the rates of radiative decay. Because these silver island surfaces are very heterogeneous, we are hopeful that larger increases in intensity and photostability can be obtained for probes situated at an optimal distance from the ideal island surfaces.

Keywords

fluorescence; two-photon excitation; multiphoton; photostability; radiative rate; surface plasmon resonance; radiative decay engineering; metal-enhanced fluorescence

INTRODUCTION

Gold and silver nanoparticles exhibit strong absorption bands that are absent in the bulk metals. These absorption bands, which are known as the surface plasmon resonance, result in strong absorption and scattering and create an enhanced local electromagnetic field near the surface of the particles. The plasmon resonances are highly dependent on the size and shape of the metal nanoparticles and the dielectric properties of the surrounding environment.[1] These near field enhancements have given rise to surface-enhanced spectroscopies such as surface-enhanced Raman spectroscopy (SERS), surface-enhanced resonant Raman scattering (SERRS), and surface-enhanced fluorescence (SEF). A great deal of research has been focused on SERS and SERRS for understanding surface phenomena and their analytical and bioanalytical applications.[2–4]

In comparison with SERS and SERRS, SEF has been explored much less. Unlike SERRS and SERS, the optimal SEF signal occurs at a certain distance from the nanoparticle surface. The fluorophores in direct contact with the metal islands are quenched. Early theoretical and

Correspondence to: B. P. Maliwal (cfs@cfs.umbi.umd.edu).

experimetal work using both rough film surfaces and particles suggested that there is a distance-dependent enhancement of the fluorescence intensity that was more pronounced for lower quantum yield probes. This enhancement is accompanied by a significantly reduced fluorescence lifetime. The phenomena of increased intensities with decreased lifetimes suggest an increased radiative rate for the affected fluorophores. Furthermore, the increased rates of energy transfer were predicted from theoretical considerations because of interactions of donors and acceptors with the plasmon resonance.[5–12] More recent experiments using Langmuir–Blodgett (LB) films have shown a distance-dependent enhancement of the fluorescence of spatially localized probes.[13–16] There are also reports of enhanced fluorescence from monolayers of fluorophores attached to proteins and the distance dependence of the enhancement[17,18] and reports of potential bioanalytical applications. [19–21] It should be noted that near field scanning optical microscope studies have shown the presence of a highly enhanced localized plasmon resonance field near sharp tips and the resulting enhanced one-[22] and two-photon absorption,[23,24] as well as greatly accelerated resonance energy transfer.[25]

In our laboratory we verified SEF and its inverse dependence on the quantum yield of probes in experiments where a small volume of the probe was sand-wiched between two quartz slides that were coated with heterogeneous silver island films. We further confirmed earlier observations of associated lowering of lifetimes.[26,27] Surprisingly, we were able to observe silver island enhanced intrinsic fluorescence from nucleic acids that have very low quantum yields.[28] We were also able to confirm predictions of enhanced energy transfer rates,[27] and we observed the expected highly enhanced two-photon excitation that is attributable to the presence of silver island surface films.[29] The photostability of the fluorescent probes appeared to increase in the presence of silver islands, which has significant practical implications. The phenomenon of SEF, which has significantly higher intensity for both one-photo and multi-photon excitation and higher total photon output, stability, and energy transfer over much longer distances, can result in new applications of fluorescence in biomedical research and diagnostics.

To date, our published experiments have been conducted on probes in free solution between silver island films about 1 μm apart. These observations included both slightly affected and largely unaffected populations. To characterize SEF where the fluorophores are spatially localized, we adapted a BSA–biotin–avidin system used by Hoshi et al.[30] and Sokolov et al. [18] In this system biotinylated BSA is adsorbed to silver island films to create a monolayer base. To this base are bound avidin molecules labeled with fluorophores. This results in a population of fluorophores localized about 5–12 nm from the silver island surfaces. We examined the fluorescence intensity with one- and two-photon excitation, the photostability with one-photon excitation, and the fluorescence lifetimes of the affected molecules.

MATERIALS AND METHODS

All common chemicals, 3-aminopropyltriethoxysilane (APS), biotinylated BSA, and avidin were purchased from Sigma–Aldrich. The amine reactive forms of the fluorophores Pacific Blue succinimidyl ester, Lissamine rhodamine sulfonyl chloride, Texas Red sulfonyl chloride, and Malachite Green isothiocyanate were purchased from Molecular Probes. The absorption spectra were collected on a Hewlett–Packard VectraXM series 3 UV–visible spectrophotometer. The steady-state fluorescence in cuvettes was measured with a Varian Cary Eclipse. Front face measurements of the coated slides were performed on a SLM 8000 spectrofluorometer.

Labeling of Avidin

Typically, 1.5–2 mg of avidin was dissolved in 1–1.5 mL of 0.2*M* bicarbonate buffer (pH 9.0) and mixed with 20–30× amounts of reactive fluorophore in a small amount of dimethyl formamide (final concentration ≤ 10%). The reaction was allowed to proceed for 3–6 h and the labeled protein was separated from the unreacted probe by passing it over a Sephadex G-25 column.

Preparation of Silver Islands on Quartz Slides

The microscope quartz slides were first cleaned overnight with a mixture of concentrated sulfuric acid and 30% hydrogen peroxide (10:1 v/v). The slides were washed thoroughly with deionized distilled water and dried. These clean slides were soaked for 5 min in a 1% APS solution and washed. The details of silver deposition were described in earlier publications.[27,28] Half of each slide was coated with silver islands and the other half was not silvered.

Preparation of Labeled Protein Monolayers

We used an adaptation of the method of Hoshi et al.[30] and Sokolov et al.[18] The quartz slides with the silver islands were first exposed to 250 μL of 5 μ*M* biotinylated BSA for at least 16 h. The coated quartz slides were thoroughly washed to remove all of the free biotin–BSA. The slides were then further equilibrated for at least 1 h with 250 μL of 2 μ*M* labeled avidin in 1 m*M* HEPES and 0.1*M* NaCl (pH 7.5). The slides were again thoroughly washed with buffer to remove any unbound avidin. Two such coated quartz slides with the islands facing each other were assembled and used for all the fluorescence experiments.

Fluorescence Measurements on Labeled Avidin Coated Quartz Slides

Both the steady-state and frequency-domain measurements were carried out using front face illumination. The excitation was vertically polarized and the emission was observed through a vertical polarizer in the steady-state measurements. Magic angle observation was used in the emission path for the frequency-domain measurements. The excitation sources were a doubled Ti-sapphire for Pacific Blue (395 nm) and a dye laser for Lissamine (570 nm), Texas Red (580 nm), and Malachite Green (600 nm). The frequency-domain data were analyzed as a sum of exponential components,

$$I(t)=\Sigma\,\alpha_i \exp(-t/\tau_i) \tag{1}$$

where α_i is the amplitude and τ_i is the decay time ($\Sigma\alpha_i = 1.0$). The average lifetime, which is the average time the fluorophore remains in the excited state, is given by

$$\overline{\tau}=\frac{\Sigma\,\alpha_i\tau_i^2}{\Sigma\,\alpha_i\tau_i}=\Sigma\,f_i\tau_i \tag{2}$$

where

$$f_i=\frac{\alpha_i\tau_i}{\sum_j \alpha_j\tau_j} \tag{3}$$

is the fractional contribution of each component to the steady-state data. The amplitude-weighted lifetime is given by

$$\langle \tau \rangle = \Sigma\, \alpha_i \tau_i \tag{4}$$

This value represents the area under the decay curve.

The quantum yields (QYs) were measured on samples with less than 0.02 optical density (OD). The slit widths were 2.5 nm for the excitation and 5 nm for the emission. For reference we used either quinine sulfate in sulfuric acid (QY = 0.55) or rhodamine B in water (QY = 0.48).

Theory

Following excitation a fluorophore in free space can either emit a photon with a radiative deactivation rate (Γ) or return to the ground state by a nonradiative deactivation rate (k_{nr}). For simplicity we are omitting the transitions to the triplet state and chemical processes leading to photodegradation. The quantum yield (Q) and lifetime (τ) of the fluorophore is given by

$$Q = \frac{\Gamma}{\Gamma + k_{nr}} \tag{5}$$

$$\tau = \frac{1}{\Gamma + k_{nr}} \tag{6}$$

The presence of nanosized noble metal particles in the proximity of a fluorophore can affect its fluorescence in two ways:

1. Illumination at the plasmon absorption of the nanosize metal particle creates an enhanced near-field intensity (I_m) that results in higher fluorescence because of increased rates of excitation. We define the excitation rate enhancement factor as the ratio of the enhanced excitation intensity in the presence of metal particles (I_{enh}) and the excitation intensity (I) in the absence of particles ($G_{exc} = I_{enh}/I$).
2. Interactions between the plasmon band and the fluorophore dipole influence both the nonradiative and radiative deactivation rates. The new radiative rate is given by $\Gamma_m = N_r\Gamma$, and the nonradiative rate is given by $k_{nr}{}^m = N_{nr}k_{nr}$. We are not assuming any correlation between the enhancement factors N_r and N_{nr}.

The fluorescence quantum yield (Q_m) and lifetime (τ_m) in the presence of metal particles are given by

$$Q_m = \frac{N_r\Gamma}{N_r\Gamma + N_{nr}k_{nr}} = \frac{\Gamma_m}{\Gamma_m + k_{nr}^m} \tag{7}$$

$$\tau_m = \frac{1}{N_r\Gamma + N_{nr}k_{nr}} = \frac{1}{\Gamma_m + k_{nr}^m} \tag{8}$$

The presence of the metal particles will change both the emission quantum yield and the fluorescence lifetime. The change in the quantum yield is described by the emission factor (G_{qy}) and the change in the fluorescence lifetime by the lifetime factor (G_τ):

$$G_{qy}=\frac{Q_m}{Q}=\frac{N_r(\Gamma+k_{nr})}{N_r\Gamma+N_{nr}k_{nr}}=N_r\frac{\tau_m}{\tau} \tag{9}$$

$$G_{\tau}=\frac{\tau_m}{\tau}=\frac{\Gamma+k_{nr}}{N_r\Gamma+N_{nr}k_{nr}} \tag{10}$$

Both radiative N_r and nonradiative N_{nr} factors can have a significant effect on the fluorescence emission. The relative contributions of these factors will depend on the separation and the relative orientation between the fluorophore and the metal particles. For very small separations, the $N_{nr}k_{nr}$ value will probably dominate and fluorescence quenching is expected. For larger separations the value of $N_{nr}k_{nr}$ rapidly decreases and $N_r\Gamma$ is expected to become the dominant factor, resulting in fluorescence enhancement. It is intuitive that the maximum value of the quantum yield enhancement factor cannot exceed a value $G_{qy} = 1/Q$ (when $N_r, \rightarrow \infty$, $Q_m \sim 1$) that corresponds to a decrease in the fluorescence lifetime to zero. We expect a significant emission enhancement factor for weak fluorophores ($Q \lll 1$) and smaller effects for higher quantum yield fluorophores.

In the cases of both low and high quantum yield fluorophores the fluorescence intensity can also be increased by a change in the excitation rate (G_{exc}). It is important to stress that the observed fluorescence enhancement ($G_{fl} = G_{exc}G_{qy}$) reflects the changes in both the excitation and decay rates. For this simplified model, there are three independent variables that affect the fluorescence observed in the presence of metal particles: G_{exc}, N_r, and N_{nr}. To solve such a system it is necessary to have three independent experiments. If we can independently measure the fluorescence lifetimes, based on Eqs. (7)–(10) we obtain for the one-photon excitation process

$$G_{fl}^{(1)}=G_{exc}\cdot G_{qy}=G_{exc}N_r\frac{\tau_m}{\tau} \tag{11}$$

If the lifetimes are measured, the observed enhancement of the fluorescence now depends on two variables, G_{exc} and N_r [eq. (11)]. In practice, the fluorescence enhancement ($G_{fl}^{(1)}$) is not enough to determine whether the measured enhancement is due to the field enhancement (G_{exc}) or to the emissive rate and/or quantum yield enhancement (N_r and/or G_{qy}). In order to overcome this problem, we used two-photon excitation.

The two-photon excitation process depends on the squared power of the excitation intensity, but it leads to the same excited state as one-photon excitation. The fluorescence lifetimes do not depend on the mode of excitation. Because it is the excited molecule that interacts with the metal nanoparticle, it is reasonable to assume that the enhancement factor is the same for one- and two-photon excitation. By analogy to Eq. (11), one can calculate the fluorescence enhancement for two-photon excitation ($G_{fl}^{(2)}$):

$$G_{fl}^{(2)}=G_{exc}^2\cdot G_{qy}=G_{exc}^2N_r\frac{\tau_m}{\tau} \tag{12}$$

Dividing (12) by (11) leads to very simple relation between the observed fluorescence enhancement for one- and two-photon excitation:

$$\frac{G_{\mathrm{fl}}^{(2)}}{G_{\mathrm{fl}}^{(1)}}=G_{\mathrm{exc}} \tag{13}$$

Thus, by employing these three measurements (the fluorescence enhancement with one- and two-photon excitation and the fluorescence lifetimes), we have a simple way of evaluating all enhancement factors in the presence of metal particles.

RESULTS AND DISCUSSION

Avidin Deposition

In our experiments the fluorescence intensity will be proportional to the amount of labeled avidin bound to the unsilvered and silvered slides. Hence, we considered the extent of avidin binding to both types of slides. We measured the adsorption of avidin to the deposited BSA–biotin base layer on the unsilvered and silver island coated quartz slides by measuring the absorption between 200 and 240 nm. Because of the size of the tetramer (515 peptide bonds), avidin has a large molar extinction of about 1,500,000 cm^{-1} M^{-1} at 210 nm. The ODs were around 0.005–0.006 at 210 nm for both the bare and silver deposited slides. These absorbance values suggest complete coverage with BSA as found in earlier reports.[18,30] The differences in the absorbance values between the bare quartz and the island deposited surfaces are small and there is a variable baseline due to silver island absorption. Using these values, an upper limit on the excess bound avidin on the silver deposited side is less than a factor of 2, if there is an excess. We calculated the excess surface area due to the silver islands. For a semispherical island with a radius of 50 nm and interisland spacing of 150 nm [a conservative assumption because all our atomic force microscopy (AFM) images show considerably more spacing], the islands will increase the total area by less than 10%. Therefore, all the intensity observations that follow reflect the surface-enhanced phenomena and not differences in the amount of bound avidin molecules.

Silver Islands

The island deposited slides had an OD of 0.30–0.35. From visual inspection it was obvious that we achieved a significantly dense island population. Based on the AFM images for a range of island preparations,[27–29] we expect there should be gaps/cavities of a minimum of hundreds of nanometers between these islands. The colloidal silver deposits exist as heterogeneous islands of various shapes and sizes, not as a continuous mirror.

Extent of Labeling and Quantum Yields in Cuvette

The extent of the labeling was calculated from the molar extinctions of avidin at 280 nm, the respective probes at their absorption maxima, and the absorption of the probes at 280 nm. The calculated number of probes are 14 for Pacific Blue, 4.5 for Lissamine, 2.5 for Texas Red, and 2.5 for Malachite Green molecules per avidin tetramer. The respective absorption and emission maxima of the labeled avidin in buffer were 395 and 458 nm for Pacific Blue, 573 and 595 nm for Lissamine, 590 and 620 nm for Texas Red, and 630 and 655 nm for Malachite Green. The quantum yields in cuvettes for the labeled avidin in the presence of fourfold BSA–biotin were 0.20 for Pacific Blue, 0.16 for Lissamine, 0.08 for Texas Red, and <0.001 for Malachite Green. These quantum yields are significantly lower than those observed for free probes in solution. It is not unusual that fluorophores are significantly quenched when attached to a protein surface.

Enhanced Fluorescence for Labeled Avidin Monolayers

The emission spectra of the Pacific Blue labeled avidin monolayer on bare and silver island deposited quartz slides are shown in Figure 1(a). The coumarin probe shows an emission maxima around 460 nm and the shape of the spectrum is the same on both surfaces. We observed an enhancement factor of about 28 for this probe that is due to silver islands. This value is a global average for the whole slide, and it was calculated by scanning at several different sites. The calculated value includes corrections for inner filter effects at both the excitation and emission wavelengths. The results for Lissamine, Texas Red, and Malachite Green labeled avidin monolayers are shown in Figure 1(b). We did not observe any significant distortion in the emission spectra in any of these probes. The respective average enhancement factors are 16, 46, and 80 for these three probes. The most enhanced Malachite Green is also the fluorophore with the lowest quantum yield.

These fluorescence enhancements are more pronounced than those seen by Sokolov and coworkers[18] with fluorescein on similar BSA–biotin–avidin mono-layers in the presence of nonaggregated silver colloid film surfaces. They also observed higher enhancement with a weaker fluorophore NBD [6-(*N*-(7-nitrobenz-2-oxa-1,3-diazol-4-yl)amino)hexanoate] in an antibody–antigen system using the same silver colloid film surfaces. Aroca et al.[13–16] used LB films and observed up to 50-fold enhanced fluorescence in the presence of silver islands with several probes. There are reasons for believing that these enhancement factors are a lower limit to what can be achieved. Our silver deposits are highly heterogeneous and we see an average over a range of sizes and shapes of islands. Recent research on the intrinsic surface-enhanced Raman properties of single Ag and Au nanoparticles suggests that a small fraction of colloidal particles show extremely large enhancements. [31–33] The same is likely to be true for silver colloids/islands SEF. The fluorescence enhancement depends on the size, shape, spacing between the islands, distance of the probe from the surface, and strength of interactions between the metal surface and the probe. With improved fabrication, it should be possible to realize far greater fluorescence enhancement factors.

Enhanced Photostability

We also studied the photostability of Pacific Blue, Lissamine, and Texas Red labeled avidin monolayers in the presence of silver island surfaces. The excitation power was less than 1 mW in all experiments. Each probe was examined with the same incident intensity on silver islands and on quartz slides. However, the absolute power levels were different for each probe because the aim was to find experimental conditions in which we could observe bleaching on the bare quartz slide. The results are shown in Figure 2. For the purpose of comparison, we have normalized the intensity to 1 for both the silver islands and the bare quartz. In each case the emission intensity is significantly higher in silver island films. In all three cases we observe a modest increase in photostability in the presence of silver islands. One of the factors that probably contributes to this enhanced stability is shortened lifetimes for the affected probes (see below). As the fluorophores spend less time in the excited state they can undergo more excitation– deexcitation cycles prior to photodecomposition. Recalling that the time-zero intensities are much higher with the silver islands, the area under these curves and hence the number of observable photons per fluorophore are dramatically increased. That is, because the rate of photobleaching is the same or lower in the presence of the silver island films, the number of observable photons per fluorophore is increased by the enhancement factors shown in Figure 1. The only other report of enhanced stability besides our own[27] is a recent publication by Ditlbacher et al.[34] From a practical perspective, better stability will be a major advantage for applications such as microscopy or DNA arrays where high excitation powers are used and bleaching/photo-degradation is a problem.

Two-Photon Excitation

The two-photon excitation of Pacific Blue, Lissamine, and Texas Red labeled avidins was also measured, and the results are shown in Figure 3. We observe an enhancement of about 200-fold in the case of Pacific Blue labeled avidin. Because we are unable to distinguish the fluorescence from the background on the quartz, there is significant uncertainty in the absolute number for the enhancement. In the Lissamine and Texas Red the observed enhancements are greater than 200-fold because the intensities on quartz are too weak to measure. The relative intensities of Lissamine and Texas Red are significantly lower than that seen for Pacific Blue. Part of the reason may be that we have an optimal wavelength in the coumarin derivative Pacific Blue[35] whereas the maxima for the other two probes are outside the wavelength range of the-Ti-sapphire laser (780–850 nm). Further, because the coumarin absorption and emission maxima and the plasmon absorption maximum coincide, there is likely to be stronger interaction between the surface plasmon and this probe.

These results are consistent with our earlier observations with several probes in solution near silver island surfaces,[29] which had enhanced two-photon excitation attributable to the presence of an enhanced plasmon field near a nanosized metal tip,[23,24] and total internal reflection measurements. What is noteworthy is the magnitude of the two-photon enhancement due to plasmon resonance.

Fluorescence Lifetime Measurements

We also measured the intensity decays for all four probes using front face illumination. A representative example of the frequency-domain response of Texas Red labeled avidin on quartz and silver island surfaces is shown in Figure 4(a). A dramatic decrease in the lifetime is obvious from the shift of the frequency response to higher frequencies. Figure 4(b) presents the calculated time- dependent decays for the system. The more rapid decay near the islands is apparent.

The results of a multicomponent analysis for the other labeled avidins are presented in Table I. On quartz the fluorescence decay was monoexponential for the coumarin derivative with a lifetime of about 0.63 ns. Both the Lissamine and Texas Red fluorescence intensity decays were heterogeneous and could be described by a sum of three lifetimes. The average lifetimes were 1.46 and 1.04 ns and the amplitude-weighted lifetimes were 0.30 and 0.51 ns for two respective probes. In the presence of silver island surfaces there was a significant reduction in the lifetimes for all three fluorophores. The intensity decays on the silver island surfaces are dominated by components below 100 ps. The average lifetimes were 0.086, 0.102, 0.04, and 0.003 ns for Pacific Blue, Lissamine, Texas Red, and Malachite Green, respectively. The respective amplitude-weighted lifetimes were 0.086, 0.042, 0.014, and 0.003 ns. The general trend is for a larger decrease in lifetime with greater intensity enhancements. We also analyzed data for associated intensity decays to see if any unaffected population is still present in the silver island samples. The analysis suggests that there is essentially no such population. Because the distances between the islands on each quartz surface are 100s of nanometers, these results would suggest that plasmon resonance is active at such distances and affects the probes bound to the surfaces between the islands. Alternatively, the emission may be dominated by the more intense fluorescence from probes near the silver particles.

The significantly reduced lifetime values have at least two major implications. The shortened lifetime should result in higher photostability. In addition, a shorter lifetime will result in a significantly higher number of photons per unit time under light saturation excitation conditions. Both of these properties will allow shorter exposure time or higher signal to noise for a comparable exposure time.

Calculation of Enhancement Factors

We can calculate the excitation enhancement factor from the relative enhancements seen with one- and two-photon excitation [Eq. (13)]. We observed enhancements of 28 for one-photon and 235 for two-photon excitations of Pacific Blue. This gives us an excitation enhancement of 8.4. Assuming the enhancement factor for two-photon excitation is near 200-fold for Lissamine and Texas Red, the excitation enhancement factors are 12- and 4-fold, respectively.

These excitation enhancement factors, along with Eq. (11) and the amplitude-weighted lifetime in Table I, can be used to calculate the relative increase in the radiative decay rates. These calculations result in G_{exc} values of 25, 9.5, and 418 for Pacific Blue, Lissamine, and Texas Red, respectively (Table II). Recognizing the unknown intensities for two-photon excitation on quartz (Fig. 3), we believe there is an average 25-fold increase in Γ.

We can also estimate the relative increase in the radiative decay rates from the lifetimes and quantum yields. In the absence of silver the radiative decay rate is given by

$$\Gamma = Q/\langle\tau\rangle \tag{14}$$

We used the amplitude-weighted lifetime because we believe it provides a more realistic estimation of Γ than the average lifetime, which is heavily weighted toward the longest decay time in a multiexponential decay. These values are summarized in Table II. The calculation is more complex in the presence of silver islands because the quantum yields near the silver are not known. Because the observed increases in intensity (Fig. 1) are larger than $1/Q$, that is, the apparent quantum yields are higher than unity, we assumed these quantum yields were 1.0. These calculations indicate the radiative decay rates are increased by 35-, 45-, and 455-fold for Pacific Blue, Lissamine, and Texas Red, respectively. We stress that these results must be recognized as qualitative, but we suggest that silver particles result in both increased excitation and larger radiative decay rates of nearby fluorophores.

CONCLUSION

Fluorescence is enhanced in the proximity of metallic silver particles. The optimal enhancement depends upon the distance and the spectral properties of the probe and how efficiently it interacts with the surface plasmon. Because the surface plasmon depends on the size, shape, and dielectric environment of the colloid particles, it should be possible to optimize the interaction for a given fluorophore and metal. The enhanced intensity is accompanied by a reduced lifetime near the nanometer aggregated colloid surface. One of the implications of these changes is a greater signal from a fluorescent probe leading to higher sensitivity and the ability to detect the fluorescent signal at lower concentrations. Furthermore, reduced lifetimes will allow the use of higher excitation powers. Similarly, a significantly enhanced multiphoton signal is also promising in extending the use of metal particles for localized excitation in samples, cells, or tissues.

One goal in the development of fluorescent probes has been to find ways to maintain high quantum yields after the probe is coupled to a protein surface. Frequently, the covalent attachment results in significant quenching. A related phenomenon is self-quenching as the probe density increases. The presence of silver colloid nanoparticles may overcome both of these limitations. In practical terms it will allow for greater labeling and the option to use a significantly larger base of available probes. The initial quantum yield of a fluorophore will be much less important, and a low quantum yield may be an advantage if the goal is to detect fluorophores bound near metallic particles. Another promising area is combining enhanced fluorescence due to silver islands with an application that also enhances the local field such as

evanescent waves in total internal reflection or surface plasmon resonance.[19,20] Such a combination may result in larger signals, a localized detector, and increased sensitivity for both one-photon and multiphoton excitation.

Acknowledgments

The authors acknowledge the support of this work by the National Institute of Biomedical Imaging and Bioengineering and the National Center for Research Resources.

Contract grant sponsor: National Institute of Biomedical Imaging and Bioengineering; contract grant number: NIH-EB00682.

Contract grant sponsor: National Center for Research Resource; contract grant number: RR-08119.

REFERENCES

1. Kreibig, U.; Volmer, M. Optical Properties of Metal Clusters. New York: Springer; 1995.
2. Moskovits M. Rev Mod Phys 1985;47:783–825.
3. Campion A, Kambhampati P. Chem Soc Rev 1998;27:241–250.
4. Kneipp K, Kneipp H, Itzkan I, Dasari RR, Feld MS. Chem Rev 1999;99:2957–2975. [PubMed: 11749507]
5. Kuhn H. J Chem Phys 1970;53:101.
6. Drexhage, KH. Progress in Optics. Wolf, E., editor. Vol. Vol. XII. Amsterdam: North-Holland; 1974. p. 163-232.
7. Chance RR, Prock A, Silbey R. Adv Chem Phys 1978;37:1–65.
8. Gersten J, Nitzan A. J Chem Phys 1981;75:1139–1152.
9. Weitz DA, Garoff S, Gersten JI, Nitzan A. J Chem Phys 1983;78:5324–5338.
10. Leitner A, Lippitsch ME, Draxler S, Riegler M, Aussenegg FR. Appl Phys B 1985;36:105–109.
11. Das PC, Metiu H. J Phys Chem 1985;89:4680–4689.
12. Kummerlen J, Leitner A, Brunner H, Aussenegg FR, Wokaun A. Mol Phys 1993;80:1031–1046.
13. DeSaja-Gonzalez J, Aroca R, Nagao Y, Desaja JA. Spectrochim Acta A 1997;53:173–181.
14. Tarcha PJ, DeSaja-Gonzalez J, Rodriguez-Llorente S, Aroca R. Appl Spectrosc 1999;53:43–48.
15. Constantino CJL, Aroca RF. J Raman Spectrosc 2000;31:887–890.
16. Antunes PA, Consantino CJL, Aroca RF, Duff J. Langmuir 2001;17:2958–2964.
17. Chumanov G, Sokolov K, Gregory BW, Cotton TM. J Phys Chem 1995;99:9466–9471.
18. Sokolov K, Chumanov G, Cotton TM. Anal Chem 1998;70:3898–3905. [PubMed: 9751028]
19. Attridge JW, Daniels PB, Deacon JK, Robinson GA, Davidson GP. Biosens Bioelectron 1991;6:201–214. [PubMed: 1883601]
20. Lieberman T, Knoll W. Colloid Surface A 2000;171:115–130.
21. Stich N, Gandhum A, Matushin V, Mayer C, Baker G, Schalkhammer T. J Nanosci Nanotechnol 2001;1:397–405. [PubMed: 12914081]
22. Hamann HF, Kuno M, Gallagher A, Nesbitt DJ. J Chem Phys 2001;114:8596–8609.
23. Sanchez EJ, Novotny L, Xie XS. Phys Rev Lett 1999;82:4014–4017.
24. Kawata Y, Xu C, Denk W. J Appl Phys 1999;85:1294–1301.
25. Fiurasek J, Chernobrod B, Prior Y, Avebukh ISh. Phys Rev B 2001;63:405–420.
26. Lakowicz JR. Anal Biochem 2001;298:1–24. [PubMed: 11673890]
27. Lakowicz JR, Shen Y, D'Auria S, Malicka J, Fang J, Gryczynski Z, Gryczynski I. Anal Biochem 2002;301:261–277. [PubMed: 11814297]
28. Lakowicz JR, Shen Y, Gryczynski Z, D'Auria S, Gryczynski I. Biochem Biophys Res Commun 2001;286:875–879. [PubMed: 11527380]
29. Gryczynski I, Malicka J, Shen Y, Gryczynski Z, Lakowicz JR. J Phys Chem 2002;106:2191–2195.
30. Hoshi T, Anzai J, Osa T. Anal Chem 1995;67:770–774. [PubMed: 7702192]

31. Nie S, Emory SR. Science 1997;275:1102–1107. [PubMed: 9027306]
32. Kneipp K, Wang Y, Kneipp H, Perelman LT, Itzkan I, Dasari RR, Feld MS. Phys Rev Lett 1997;78:1667–1670.
33. Zeisel D, Deckert V, Zenobi R, Vo-Dinh T. Chem Phys Lett 1998;283:381–385.
34. Diltbacher H, Felidj N, Krenn JR, Lamprecht B, Leitner A, Aussenegg FR. Appl Phys B 2001;73:373–377.
35. Fischer A, Cremer C, Stelzer EHK. Appl Opt 1995;34:1989–2003.

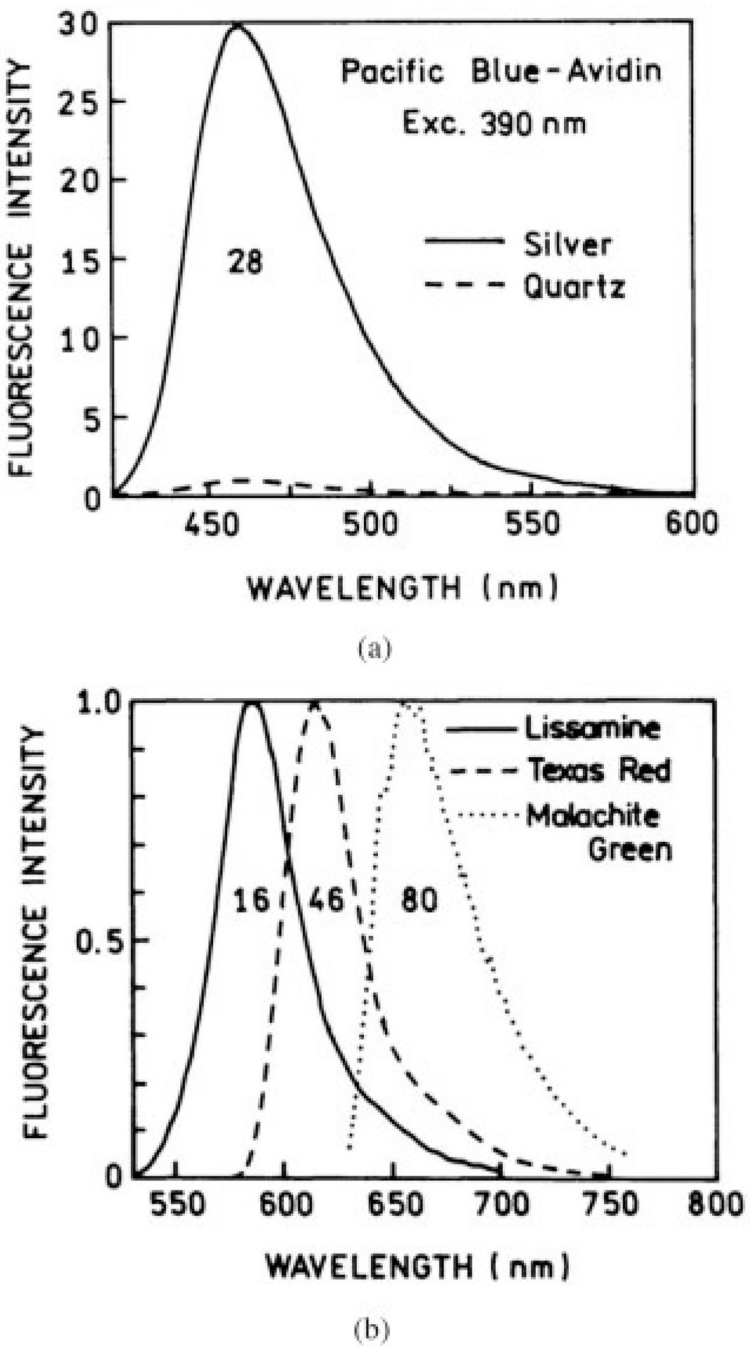

FIGURE 1.

Emission spectra of labeled avidin molecules bound to BSA-coated silver island films. The numbers indicate the relative intensities of labeled avidins on silver island films as compared to quartz.

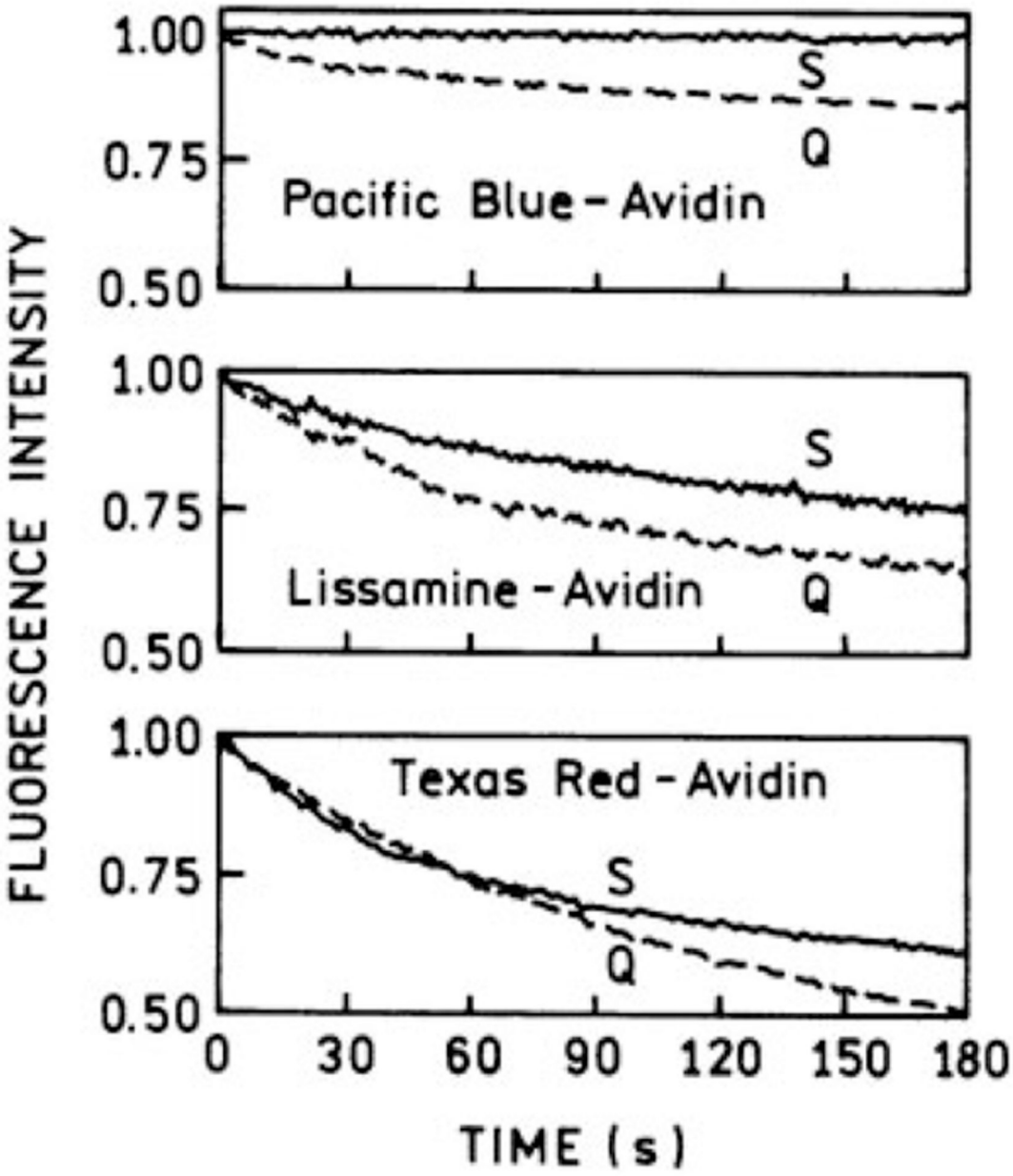

FIGURE 2.
Comparisons of the photostability of labeled avidins in the presence (S) and absence (Q) of silver island surfaces. The intensities at time zero are normalized to 1.

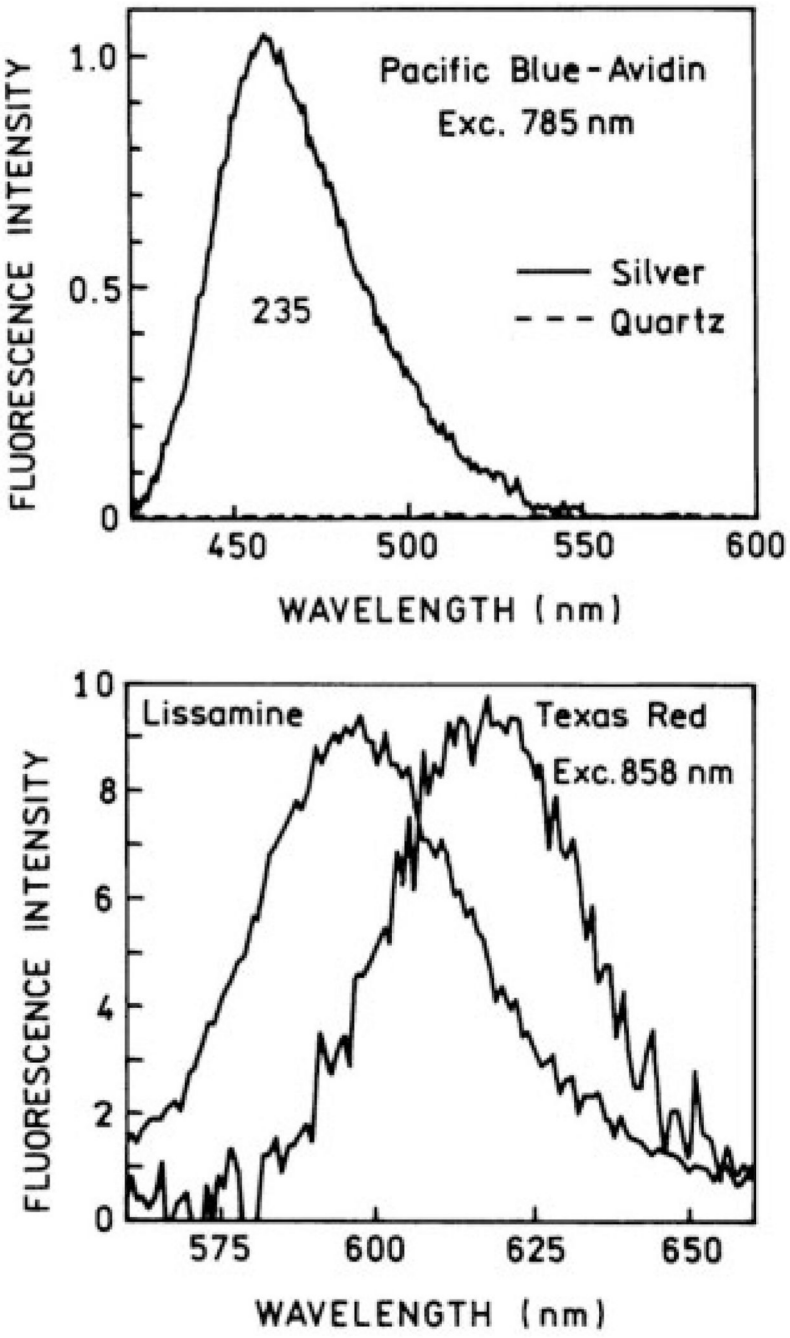

FIGURE 3.
Emission spectra of the labeled avidins with two-photon excitation in the presence of silver island films or bare quartz.

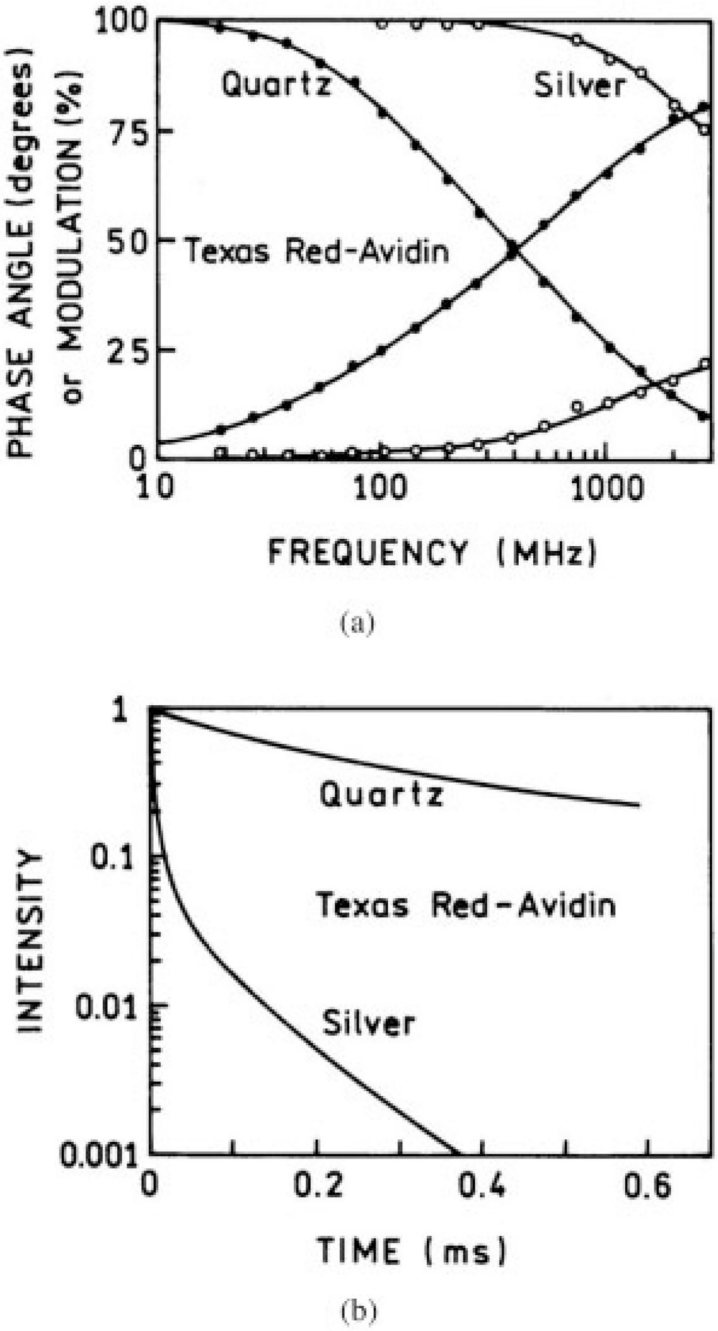

FIGURE 4.

(a) The frequency-domain intensity decays of Texas Red labeled avidin on the silver islands and the quartz surface. (b) The reconstructed time-domain decay.

Table I

Multicomponent Analysis of Fluorescence Intensity Decays of Labeled Avidins

Probe	τ_1 (ns)	τ_2 (ns)	τ_3 (ns)	α_1	α_2	α_3	f_1	f_2	f_3	$\bar{\tau}$ (ns)	$\langle\tau\rangle$ (ns)	χ_R^2
Quartz												
Pacific Blue	0.627	—	—	1.00	—	—	1.00	—	—	0.63	0.63	1.30
Lissamine	3.04	0.457	0.076	0.041	0.227	0.682	0.41	0.42	0.17	1.46	0.30	2.12
Texas Red	2.44	0.871	0.261	0.053	0.226	0.721	0.25	0.38	0.37	1.04	0.51	1.58
Silver Islands												
Pacific Blue	0.086	—	—	1.00	—	—	1.00	—	—	0.086	0.86	0.69
Lissamine	0.243	0.045	0.019	0.055	0.422	0.522	0.32	0.45	0.23	0.102	0.042	1.82
Texas Red	—	0.087	0.009	—	0.063	0.937	—	0.40	0.60	0.040	0.014	2.10
Malachite Green	—	—	0.003	—	—	1.00	—	—	1.00	0.003	0.003	1.31

The intensity decays are analyzed in terms of the multiexponential model,

$$I(t)=\sum \alpha_i \exp(-t/\tau_i)$$

where α_i is the amplitude and τ_i is the decay time. The average lifetime is given by

$$\bar{\tau}=\sum \alpha_i \tau_i^2 / \sum a_i \tau_i$$

The amplitude-weighted lifetime is given by

$$\langle\tau\rangle = \sum a_i \tau_i / \sum \alpha_i$$

Table II

Calculated Enhancement Factor for Labeled Avidin

Probe	$G_{fl}^{(1)}$	$G_{fl}^{(2)}$	G_{exc}	Γ (ns^{-1})[a]	Γ_m(ns^{-1})[a]	N_r
Pacific Blue	28	235	25	0.32	11[b]	35
Lissamine	16	200[c]	9.5[c]	0.53	23[b]	45
Texas Red	46	200[c]	418[c]	0.16	71[b]	455

[a] Calculated using $\Gamma = Q/\langle\tau\rangle$.

[b] Calculated assuming the quantum yield =1.0 on the silver island films.

[c] Calculated assuming two-photon excitation displays a 200-fold increase in probe fluorescence on the silver island films.